Published in final edited form as:
Nat Med. 2009 October ; 15(10): 1202–1207. doi:10.1038/nm.2023.

Inhibition of calpain increases LIS1(PAFAH1B1) and partially rescues *in vivo* phenotypes in a mouse model of lissencephaly

Masami Yamada[1,*], **Yuko Yoshida**[1,*], **Daisuke Mori**[1], **Takako Takitoh**[1], **Mineko Kengaku**[2], **Hiroki Umeshima**[2], **Keizo Takao**[3,4,5], **Tsuyoshi Miyakawa**[3,4,5], **Makoto Sato**[6,7], **Hiroyuki Sorimachi**[8], **Anthony Wynshaw-Boris**[9], and **Shinji Hirotsune**[1,#]

[1]Department of Genetic Disease Research, Osaka City University Graduate School of Medicine, Asahi-machi 1-4-3 Abeno, Osaka 545-8585, Japan

[2]Institute for Integrated Cell-Material Sciences, Kyoto University Yoshida-honmachi, Sakyo-ku, Kyoto 606-8501, Japan

[3]Division of Systems Medical Science, Institute for Comprehensive Medical Science, Fujita Health University, Toyoake, Aichi 470-1192, Japan

[4]Genetic Engineering and Functional Genomics Group, Frontier Technology Center, Kyoto University Faculty of Medicine, Yoshida-Konoe-cho, Sakyo-ku, Kyoto 606-8501, Japan

[5]Japan Science and Technology Agency, BIRD & CREST, Kawaguchi, Saitama 332-0012, Japan

[6]Division of Cell Biology and Neuroscience, Department of Morphological and Physiological Sciences, Faculty of Medical Sciences, University of Fukui, Fukui 910-1193, Japan

[7]Research and Education Program for Life Science, Faculty of Medical Sciences, University of Fukui, Fukui 910-1193, Japan

[8]Department of Enzymatic Regulation for Cell Functions (Calpain Project), The Tokyo Metropolitan Institute of Medical Science (Rinshoken), Tokyo Metropolitan Organization for Medical Research 2-1-6 Kamikitazawa, Setagaya-ku, Tokyo 156-8506, Japan

[9]Department of Pediatrics and Institute for Human Genetics, University of California, San Francisco School of Medicine, 513 Parnassus, HSE 901F, San Francisco, CA 94143-0794

Abstract

[#]Correspondence should be addressed to: Shinji Hirotsune, Shinji Hirotsune: Tel: +81-6-6645-3725, Fax: +81-6-6645-3727, shinjih@med.osaka-cu.ac.jp.
[*]These authors equally contributed to this work.

Author Contributions

Masami Yamada conducted the most of experiments and wrote the manuscript.
Yuko Yoshida conducted the most of experiments.
Daisuke Mori contributed in vivo analysis of mutant moice.
Takako Takitoh contributed to reaggregation assay of granular neurons.
Mineko Kengaku contributed to reaggregation assay of granular neurons.
Hiroki Umeshima contributed to reaggregation assay of granular neurons.
Keizo Takao contributed to behavior analysis.
Tsuyoshi Miyakawa contributed to behavior analysis.
Makoto Sato contributed to in utero injection.
Hiroyuki Sorimachi contributed to experiments regarding calpain inhibition.
Anthony Wynshaw-Boris wrote the manuscript and provided valuable suggestions.
Shinji Hirotsune conducted the most of experiments and wrote the manuscript.

Lissencephaly is a devastating neurological disorder due to defective neuronal migration. *LIS1* (or *PAFAH1B1*) was identified as the gene mutated in lissencephaly patients, and was found to regulate cytoplasmic dynein function and localization. Here, we show that more than half of LIS1 is degraded via calpain-dependent proteolysis, and that inhibition or knockdown of calpains protects LIS1 from proteolysis, resulting in the augmentation of LIS1 levels in *Lis1*+/− mouse embryonic fibroblast (MEF) cells, which leads to rescue of the aberrant distribution of cytoplasmic dynein, mitochondria and β-COP positive vesicles. We also show that calpain inhibitors improve neuronal migration of *Lis1+/−* cerebellar granular neurons. Intra-peritoneal injection of ALLN to pregnant *Lis1*+/− dams rescued apoptotic neuronal cell death and neuronal migration defects in *Lis1*+/− offspring. Furthermore, *in utero* knockdown of calpain by shRNA rescued defective cortical layering in *Lis1+/−* mice. Thus, the inhibition of calpain is a potential therapeutic intervention for lissencephaly.

Introduction

In lissencephaly patients, mutation of two genes, *LIS1* or *DCX*, account for the majority of classical lissencephaly (ILS)1–3. Consistent with an important role for this protein in neuronal migration, mice with decreased *Lis1* exhibited disorganization of cortical layers, hippocampus and olfactory bulb in dose dependent fashion, and are a good model for the human disorder4. LIS1 was first identified as a subunit of the brain platelet-activating factor acetylhydrolase (PAFAH1B1)5, but extensive studies in a variety of model organisms from bread molds to mammals led to the conclusion that LIS1 is essential for the proper regulation and localization of cytoplasmic dynein6–8. Many studies have further delineated the role of LIS1 on neuronal morphogenesis and the maintenance of cell integrity. However, no studies have addressed potential therapeutic approaches for lissencephaly, a devastating human disorder.

We previously demonstrated that LIS1 is required for anterograde transport of cytoplasmic dynein in a kinesin dependent fashion8. Interestingly, we found that a substantial fraction of LIS1 is degraded at the periphery (cortex) of the cell. We probed for molecules that were involved in LIS1 degradation using inhibitors, and found that calpain inhibitors efficiently prevented the degradation of LIS1, suggesting that LIS1 is degraded by calpain dependent proteolysis. Here, we report that inhibition of calpain rescued various phenotypes that were observed in cells and in the whole animal using our *Lis1*-deficient mice that are a good model of this disorder. Our work provides a proof-of-principle for the treatment of lissencephaly die to haploinsufficiency of LIS1, and also suggests a unique therapeutic strategy for diseases associated with haploinsufficiency.

Results

LIS1 is degraded by calpain and inhibition of calpain rescued defective distribution of cytoplasmic dynein and membranous components in the cell

First, we examined the response of LIS1 protein levels to the inhibition of calpain by ALLN using mouse embryonic fibroblast (MEF) cells4. LIS1 protein gradually increased in the *Lis1*+/− MEF cells, and reached a plateau two hours after the start of ALLN treatment (data not shown). After two hours of administration of ALLN, LIS1 protein was increased from 0.5 (where 1.0 is equivalent to wild type levels of LIS1) to 1.1 (Supplementary Fig. 1, Fig. 1a). We also examined the effect of E64d, another calpain inhibitor and obtained similar results (Fig. 1a: from 0.5 to 0.9). The amount of cytoplasmic dynein intermediate chain 1(DIC1) was also increased, suggesting that the protein stability of cytoplasmic dynein was reduced in the *Lis1* mutated cells (Fig. 1a), which may be attributed to the direct prevention of degradation of cytoplasmic dynein or the indirect stabilization through normalization of

its distribution. We also examined the effect of ALLN or E64d treatment on dorsal root ganglia (DRG) neurons, and obtained similar results in the *Lis1+/−* DRG neurons by ALLN (LIS1: from 0.4 to 0.7, DIC1: 0.8 to 1.6), and by E64d (LIS1: from 0.4 to 0.9, DIC1: 0.8 to 1.5) (Fig. 1b). In contrast, there was no significant effect of calpain inhibitors on LIS1 or DIC1 in *Lis1+/+* MEF cells or DRG neurons (Supplementary Fig. 2a, b). We next determined whether preventing the degradation of LIS1 rescued the aberrant distribution of LIS1 and cytoplasmic dynein within the *Lis1*+/− MEF cells. Treatment of *Lis1+/−* MEF cells by ALLN or E64d clearly improved the reduction of centrosomal concentration of LIS1 after 2 hours of the treatment (Supplementary Fig. 2c). In addition, the abnormal accumulation of cytoplasmic dynein around the centrosome was rescued by ALLN or E64d treatment (Supplementary Fig. 2d). These improvements were also observed in the *Lis1+/−* DRG neurons (Supplementary Fig. 2e, f), whereas there was no significant effect in *Lis1+/+* DRG neurons (Supplementary Fig. 2e, f). We next addressed whether ALLN or E64d was able to rescue the aberrant distribution of cell components transported by cytoplasmic dynein in *Lis1+/−* MEF cells. Mitochondria displayed dispersed distribution in *Lis1+/+* MEF cells. By contrast, they clustered in the perinuclear region of *Lis1+/−* MEF cells (Supplementary Fig. 2g). This aberrant clustering was rescued by ALLN or E64d treatment (Supplementary Fig. 2g). Immunofluorescence demonstrated that β-COP-positive vesicles displayed a predominantly juxtanuclear staining pattern in *Lis1+/+* MEF cells (Supplementary Fig. 2h). In *Lis1+/−* MEF cells, this juxtanuclear clustering was disrupted, and β-COP displayed punctuate clustering9 (Supplementary Fig. 2h). This aberrant distribution of β-COP positive vesicles in *Lis1+/−* MEF cells was also rescued by ALLN or E64d treatment (Supplementary Fig. 2h). These effects of calpain inhibitors were not observed in *Lis1+/+* MEF cells (Supplementary Fig. 2i–l). These observations suggest that inhibition of calpains improves the functional defects of cytoplasmic dynein in *Lis1+/−* MEF cells.

Inhibition of LIS1 degradation rescued defective migration in Lis1+/− neurons

To define the effect of calpain inhibitors on mammalian neuronal migration, we used mouse cerebellar granule neurons in an *in vitro* migration assay combined with ALLN or E64d treatment9¯12. As heterozygous loss of *LIS1* leads to lissencephaly in humans, graded reduction of *Lis1* results in increased severity of migration defects in mice4. We first examined whether inhibition of calpain might affect neuronal migration in wild type cells, and found that calpain inhibition slightly facilitated neuronal migration (Fig. 2a, b, c). We next confirmed that *Lis1*+/− cerebellar granule neurons displayed a leftward shift of the bin distribution of migration distance, and the mean distance decreased by approximately half from the wild type level (Fig. 2a, b, c). We then tested whether ALLN or E64d treatment was sufficient to rescue the migration defect in *Lis1*+/− cerebellar granule neurons. *Lis1*+/− cerebellar granule neurons in the presence of ALLN or E64d displayed a shift in migration distance bins back toward the right, with a similar distribution to that of wild type neurons (Fig. 2a, b). Quantitation of mean migration distance of cerebellar granule neurons demonstrated rescue of defective migration in *Lis1*+/− cerebellar granule neurons by ALLN or E64d treatment (Fig. 2c). Specifically, inhibition of LIS1 degradation by ALLN or E64d restored migration to 83.1% (ALLN) or 84.4% (E64d) of wild type levels in *Lis1*+/− cerebellar granule neurons. Calpain inhibitors also slightly but significantly facilitated neuronal migration in wild type cells. It was previously shown that overexpression of LIS1 facilitates neuronal migration11, so it is possible that calpain inhibition might stabilize LIS1 locally, and/or may function by other mechanisms, including modulation of focal adhesion kinase (FAK) and/or Cdk5/p35.

FAK that is a tyrosine kinase localized to focal adhesions has been shown to be critical for cell migration13,14. FAK levels are regulated by calpain-dependent cleavage15¯19. FAK is

also a physiological substrate of Cdk5 during neocortical development[20–22]. We therefore examined whether inhibition of calpain might modify distribution and/or expression of focal adhesion complex by migration assay using granular neurons, and did not observe obvious differences of distribution and expression of FAK and vinculin by inhibition of calpains (Supplementary Fig. 3a–e). While we cannot completely exclude the possibility that inhibition of calpain might modify signal transduction from focal adhesion, tour findings do not support this possibility.

Knockdown of calpain by siRNA restored LIS1 protein resulting in rescue of aberrant distribution of cytoplasmic dynein and membranous components in the cell

ALLN and E64d are broad cysteine protease inhibitors, and can inhibit other cysteine proteases other than calpain, including cathepsins and papain[23,24]. To address whether calpain is a major enzyme for the degradation of LIS1 protein, we investigated the effect siRNA against calpain. The ubiquitous calpains, μ-calpain (calpain I) and m-calpain (calpain II), are heterodimers consisting of large catalytic subunits encoded by the *Capn1* and *Capn2* genes, respectively, and the small regulatory subunit encoded by *Capns1*[23,24]. Inactivation of μ-calpain and m-calpain simultaneously by siRNA was technically challenging. Therefore, we knocked down *Capns1* by siRNA, resulting in depletion of the both of μ-calpain and m-calpain[25] (Supplementary Fig. 4a, b). After transfection of siRNA against *Capns1*, μ-calpain and m-calpain were gradually decreased over 48 hrs, and were almost undetectable after 96 hrs (Supplementary Fig. 4a, b). This decrease in calpain was associated with an increase of LIS1 and DIC1 levels in *Lis1+/−* MEFs (Fig. 3), consistent with the effects of calpain inhibitors shown above. The subcellular distribution abnormalities of LIS1 and DIC1 found in *Lis1+/−* cells was rescued by depletion of μ-calpain and m-calpain (Supplementary Fig. 4c, d). The aberrant distributions of β-COP and mitochondria were also rescued by depletion of μ-calpain and m-calpain (Supplementary Fig. 4e, f). These observations suggest that LIS1 is specifically degraded by calpain, and selective inhibition of calpain is sufficient to increase LIS1 levels for improvement of the cellular phenotypes.

Intra-peritonial administration of ALLN partially rescued apoptotic cell death and defective neuronal migration

These observations prompted us to examine whether the administration of ALLN to pregnant *Lis1+/−* dams rescued defective neuronal migration *in vivo*[4]. We first examined the effect of LIS1 protection from degradation by intraperitoneal injection of ALLN. We injected ALLN (38.3 μg/g) into E12.5 pregnant *Lis1+/−* dams, and examined LIS1 in embryonic brains by Western blotting at various times after injections. We found that LIS1 increased from one hour after injection and reached a plateau 6–12 hrs later (Supplementary Fig. 5a). The effect of ALLN decreased thereafter, and returned to the original level after 24 hrs, suggesting that ALLN is relatively short acting. Thus, we performed intraperitoneal injection of pregnant dams between E9.5–E17.5 every day, and observed cell survival and neuronal migration in the brains of *in utero* treated offspring. We previously reported a mild reduction of the density of cells in the neocortex of the *Lis1+/−* mice due to apoptotic cell death in the ventricular zone[9]. *Lis1+/−* mice displayed a reduction of brain weight compared to the wild type control pups, an effect that was partially rescued by administration of ALLN (Fig. 4a). In *Lis1+/−* mice, apoptotic cell death was increased at E15.5[9], whereas it was clearly suppressed by administration of ALLN (Fig. 4b). LIS1 is essential for neuroepithelial stem cell proliferation[4,26]. To trace proliferation of stem cells, we performed BrdU pulse labeling of E13.5 embyros, and found that BrdU incorporation was not significantly different among the four groups (Supplementary Fig. 5b). Although calpain inhibitors might facilitate proliferation of neuroepithelial stem cell in *Lis1+/−* mice, the effects on

heterozygotes may be too small to measure. Thus, we believe that suppression of apoptotic cell death more likely contributes to the rescue of brain size by ALLN.

We next examined the effect of ALLN on the cortical and hippocampal layering of neurons. *Lis1+/−* mice exhibited laminar splitting and discontinuities of pyramidal cells in the CA3 and CA2 region4 (Fig. 4c). After administration of ALLN *in utero*, *Lis1+/−* mice also displayed splitting and diffuse packing of pyramidal cells, but these defects were markedly improved (Fig. 4c, and Supplementary Fig. 5c). To examine cortical lamination, we analyzed Brn-1 immunoreactivity, to label interneurons of layer 2 and 327. In *Lis1+/−* mice, Brn-1 positive cells exhibited a broader distribution compared to *Lis1+/+* mice. Administration of ALLN resulted in a more tightly packed lamination in *Lis1+/−* mice (Fig. 4d). To confirm the morphological improvement by daily ALLN treatment *in utero*, we performed quantitative BrdU birthdating analysis. In *Lis1+/−* mice, the distribution of labeled cells was shifted downward toward the ventricular zone in the cortex, and BrdU-labeling was more diffusely localized4 (Fig. 4e). The migration defects associated with the disruption of *Lis1* were partially rescued by ALLN treatment (Fig. 4e). In migration assay using granular neurons *in vitro*, calpain inhibitors slightly but significantly facilitated neuronal migration in wild type, whereas *in utero* treament with calpain did not have a significant effect on the wild type embryo. Examination of neuronal migration *in vivo* in the embryo was performed 13–15 days after the start of injection of a calpain inhibitor, whereas the *in vitro* migration assay of granular neurons was performed 16 hr after treatment of calpain inhibitors. Over several days of migration *in vivo*, slight differences in speeds of neuronal migration may not result in detectable phenotypic difference, since once migrating neurons reach the proper position in the brain, they receive stop signals for migration28. Examination of neuronal migration *in vivo* in the embryo may not be sensitive enough for the detection of this statistically significant but small difference (73.9 μm/69.4 μm: 6.5%). In contrast, in *Lis1* heterozygous granular neurons, the difference between the absence or presence of ALLN is significant (57.7 μm/37.4 μm: 54.3%).

To examine the effect of calpain knockdown in neuronal migration *in vivo*, we introduced shRNA against calpain small subunit1 into the E14 mouse neocortex by *in utero* electroporation. ShRNA against calpain small subunit depleted the both of calpain 1 and calpain 2 as with siRNA against calpain small subunit (Supplementary Fig. 6). In P4 *Lis1+/+* mice that had been transfected with control GFP, many cells labeled in the ventricular zone migrated out towards the pial surface (Fig. 4f). By contrast, neurons in P4 *Lis1+/−* displayed defective placement, consistent with decreased motility (Fig. 4f). Inactivation of μ-calpain and m-calpain partially rescued defective neuronal migration, resulting in larger fraction of neurons that reached more superficial layers. These data are consistent with our histological examinations, and support that calpain inhibition in *Lis1+/−* embryos is effective in facilitating neuronal migration.

Intra-peritonial administration of ALLN partially rescued impaired motor behavior

Lis1+/− mice displayed abnormal behavior and impaired in the spatial learning, including hindpaw clutching responses, a rotarod test and the Morris water maze task29. Therefore, we examined whether administration of ALLN *in utero* during embryonic development of *Lis1+/−* mice (ALLN-plus group) is effective in improving motor behavior compared to untreated *Lis1+/−* mice (ALLN-minus group). Standard measurements were not significantly different between the ALLN-minus and ALLN-plus groups, including body weight and body temperature (Supplementary Table 1). *Lis1+/+* mice, ALLN-minus group and the ALLN-plus group displayed similar grip strength. Importantly, despite similar grip strength between the ALLN-minus group and the ALLN-plus group, the ALLN-plus group displayed longer time to hang on the wire before falling (Supplementary Fig. 7, Fig. 5a), suggesting that motor coordination in the ALLN-plus group was improved. Next, we

examined rotarod performance. The time that *Lis1+/+* mice and ALLN-plus group maintained their balance on the top of the rotating rod increased significantly over the six trials. However, the latency to fall for the ALLN-minus group was significantly less than that recorded for wild type mice as we previously reported29 (Fig. 5b). Importantly, impaired performance on the rotarod test in the ALLN-minus group was significantly improved in the ALLN-plus group (Fig. 5b). Finally, we analyzed gait dynamics to address quantitative neurological traits of *Lis1+/−* mice. Stride length variability of forelimbs was increased in the ALLN-minus group (Fig. 5c)30. In the ALLN-plus group, this variability was improved (Fig. 5c). Normal paw angles are ~5 degree in fore paws and ~10 degree in hind paws. More open angles of the hind paws are associated with ataxia, spinal cord injury and demeyelinating diseases31. The ALLN-minus group displayed more open angles of the fore paws (Fig. 5d), an abnormality that returned to normal angles in the ALLN-plus group. Interestingly, these aberrant gait parameters were more conspicuous in the fore paws, and less remarkable in the hind paws. Restoration of normal parameters in gait analysis also supported the functional improvement of *Lis1+/−* mice after injection of ALLN.

Discussion

In this report, we have presented proof-of-principle for a novel and potentially effective therapeutic strategy for human lissencephaly, using our *Lis1*-deficient mice that are a good model of this disorder. Therapeutic strategies for lissencephaly are a daunting consideration for several reasons. First, given the nature of lissencephaly, one would have to treat all neurons throughout development. Second, *LIS1* mutations in humans are de novo, so that detection of the disorder at an early enough time point to allow effective therapy is difficult. In spite of these difficulties, there are some advantages to considering the treatment of lissencephaly that results from *LIS1* haploinsufficiency. First, LIS1 protein is present and can potentially be manipulated, since individuals display heterozygous, not complete loss of *LIS1*. Second, there are dosage dependent effects of LIS1, so any augmentation of LIS1 protein levels will likely have a beneficial effect. Third, a great deal is known about the pathogenesis and mechanism of action of LIS1 and its pathway, so the effects of any therapeutic modality can be assessed directly with quantitative measures *in vivo* and *in vitro*.

We based this therapeutic strategy on our recent observations that LIS1 is degraded after anterograde transport to the nerve terminals in a calpain dependent fashion. Inhibition of calpain resulted in the augmentation of LIS1 protein, which led to the rescue of aberrant distribution of cytoplasmic dynein from *Lis1*-deficient mice. We further demonstrated that inhibition of calpain rescued neuronal migration from granule neurons from the *Lis1* mutants. Most importantly, we demonstrated that daily ALLN administration *in utero* was partially effective in improving the defective migration phenotypes *in vivo* in the *Lis1*-deficient mice, which was associated with improvement in motor function.

Recently, it was shown that increased LIS1 expression affects human and mouse brain development32. In our case, inhibition of calpain activity results in normalization close to the wild type levels rather than accumulation of LIS1 in excess. We believe that the restoration of more normal LIS1 levels was one reason that calpain inhibition resulted in phenotypic improvement of *Lis1+/−* mice. We cannot rule out the possibility that other effects of calpain may also play some roles in the observed phenotypic rescue, including suppression of spectrin/neurofilaments/MT breakdown, cleavage of p35, a Cdk5 activator important for neuronal migration33¯35, prevention of degradation of other proteins included in the Lis1/Ndel1/Dynein complex and/or acetylated tubulin or FAK complex18,20, which will be the subjects of further investigation.

Several problems remain and must be overcome if this promising avenue of therapy can be eventually tested in human lissencephaly, including further refinement of the use of calpain inhibitors for the effective inhibition of LIS1 degradation as well as the safe and effective delivery of such drugs for clinically effective treatment of human lissencephaly. In spite of the challenges, our work provides a potential avenue to consider therapeutic strategies for severe, early brain developmental defects such as lissencephaly due to *LIS1* mutations, as well as any other disorder that results from haploinsufficiency.

Methods

DRG preparation, culture, fluorescence recovery measurement after photobleaching (FRAP) and reaggregate neuronal migration assay

DRGs from postnatal mice were dissociated using a previously described method37. Cerebellar granule cells were isolated as described previously9,10,12 and cultured at 10^6 cells/ml for 12 hrs, resulting in uniform-sized reaggregates (100–150 μm in diameter), which were then transferred to poly-L-lysine– (Sigma-Aldrich) and laminin- (Sigma-Aldrich) treated slides and incubated for 8 hrs. Then, 10 μM ALLN (Calbiochem), 20 μM E64d (Calbiochem) or control DMSO was added and the cultures were further incubated for 16 h. Images were obtained using a 20x objective lens and images were analyzed using a confocal microscope (TCS-SP5, Leica).

BrdU birthdating study

For bromodeoxyuridine (BrdU) experiments, pregnant dams (E15.5) were injected with BrdU (50 μg/g, i.p.). Subsequently, the distribution of BrdU-positive cells was determined at P5. For pulse labeling to trace proliferation of neuroepithelial stem cell, pregnant dams (E13.5) were injected with BrdU (150 μg/g, i.p.). Subsequently, the distribution of BrdU-positive cells was determined one hour after the injection. The incorporation of BrdU in cells was detected with a mouse anti-BrdU monoclonal primary antibody (Roche) followed by an alkaline phosphatase-conjugated secondary antibody (Boehringer Mannheim). We analyzed three independent mice for each genotype.

Histological examination and immunohistochemistry

After perfusion with 4% PFA fixative, tissues from wild type and various mutant mice were subsequently embedded in paraffin and sectioned at 5 μm thickness. After deparaffination, endogenous peroxidase activity was blocked by incubating the sections in 1.5% peroxide in methanol for 20 min. The sections were then boiled in 0.01 M citrate buffer, pH 6.0, for 20 min and cooled slowly. Before staining, the sections were blocked with rodent block (LabVision) for 60 min. The sections were washed in PBS and incubated with an anti-Brn-1 antibody (Santa Cruz).

Cell culture and immunocytochemistry

Establishment of mouse embryonic fibroblast (MEF) cells was performed as previously described9,12. MEF cells were grown in D-MEM supplemented with 10% FBS. To inhibit calpain, MEF cells were incubated with 10 μM ALLN (Calbiochem), 20 μM E64d (Calbiochem) or control DMSO for 2 hrs. Cells were fixed in 4% PFA in PBS followed by permealization with 0.2% Triton X-100 in PBS. Coverslips were blocked for one hour with Block Ace (Yukijirushi) in PBS supplemented with 5% BSA, and were incubated for one hour in primary antibody, washed, and incubated for 1 hr using Alexa 546-conjugated secondary antibodies (Molecular Probes). Primary antibodies were an anti-β COP antibody (Sigma) and an anti-DIC1 antibody (Chemicon). Mitochondria were stained by MitoTracker

Green FM (Molecular Probes). The anti-calpain antibody (1D10A7) was provided from Seiichi Kawashima, which recognized conventional calpain36.

SiRNA, shRNA and transfection

Used siRNA and shRNA to target the mouse *Capns1* (calpain small subunit 1) was purchased from Sigma (MISSION® siRNA: SASI_Mm01_00127701, and MISSION™ TRC shRNA: TRCN0000087168). siRNA was transfected with Lipofectamine RNAi MAX reagents (Invitrogen, Carlsbad, CA). shRNA was *in utero* electroporation-mediated gene transfer method38,39. shRNA plasmid and pCAGGS-GFP control plasmid were dissolved in HBS (21 mM HEPES, pH 7.0, 137 mM NaCl, 5 mM KCl, 0.7 mM Na2HPO4, 1 mg/l glucose) at a final concentration of 10mg/ml together with Fast Green (final concentration 0.01%). For cotransfection, a molar ratio of 1 (pCAGGS-GFP) to 3–6 (shRNA) was used.

Behavior analysis

Forty one (25 males and 16 females) wild type, fourteen (5 males and 9 females) *Lis1+/−* mice and fifteen (12 males and 3 females) *Lis1+/−* mice that were treated *in utero* with ALLN were used for behavioral experiments. *Lis1+/−* mice had a single *Lis1* mutant allele. In this study mice were from a mixed genetic background (129SvEv×FVB). All animal experiments were carried out under protocols approved by Kyoto University. In this screen, several physical features and several motor responses of the mice were recorded including body weight and core temperature. Rotarod test was conducted as previously described40.

Eighteen (11 males and 7 females) wild type, thirteen (4 males and 9 females) *Lis1+/−* mice and fifteen (12 males and 3 females) *Lis1+/−* mice that were administrated with ALLN were used for regular behavioral experiments. Gait analysis was performed using ventral plane videography as described41. Briefly, mice were placed on the treadmill belt that moves at a speed of 24.7 cm/s. Digital video images of the underside of mice were collected at 150 frames per second. The paw area indicates the temporal placement of the paw relative to the treadmill belt. The color images were converted to their binary matrix equivalents, and the areas (in pixels) of the approaching or retreating paws relative to the belt and camera were calculated throughout each stride. Plotting the area of each digital paw print (paw contact area) imaged sequentially in time provides a dynamic gait signal, representing the temporal record of paw placement relative to the treadmill belt.

Supplementary Material

Refer to Web version on PubMed Central for supplementary material.

Acknowledgments

We thank Seiichi Kawashima for providing us an anti-calpain antibody (1D10A7)36. We thank Yoshihiko Funae, Hiroshi Iwao, Toshio Yamauch, Masami Muramatsu and Yoshitaka Nagai for generous support and encouragement. We also thank Yukimi Kira, Yoriko Yabunaka and Ryusei Zako for technical support, Hiromichi Nishimura and Keiko Fujimoto for mouse breeding, Teruko Bando for *in utero* injection and Kazuo Nakanishi for behavior study. This work was supported by Grant-in-Aid for Scientific Research from the Ministry of Education, Science, Sports and Culture of Japan from the Ministry of Education, Science, Sports and Culture of Japan to Makoto Sato and Shinji Hirotsune. This work was also supported by The Sagawa Foundation for Promotion of Cancer Research, The Cell Science Research Foundation, The Japan Spina Bifida & Hydrocephalus Research Foundation, Takeda Science Foundation, The Hoh-ansha Foundation and Knowledge Cluster Initiative (Stage-2) Research Foundation to Shinji Hirotsune, and NIH grants NS41030 and HD47380 to Anthony Wynshaw-Boris. This work was also supported by Grant-in-Aid for Scientific Research on Priority Areas -Integrative Brain Research (Shien)- from MEXT and Grant-in-Aid from Neuroinformatics Japan Center (NIJC), Japan to Tsuyoshi Miyakawa.

References

1. Reiner O, et al. Isolation of a Miller-Dieker lissencephaly gene containing G protein beta-subunit-like repeats. Nature. 1993; 364:717–721. [PubMed: 8355785]
2. Gleeson JG, et al. Doublecortin, a brain-specific gene mutated in human X-linked lissencephaly and double cortex syndrome, encodes a putative signaling protein. Cell. 1998; 92:63–72. [PubMed: 9489700]
3. Pilz DT, et al. LIS1 and XLIS (DCX) mutations cause most classical lissencephaly, but different patterns of malformation. Hum Mol Genet. 1998; 7:2029–2037. [PubMed: 9817918]
4. Hirotsune S, et al. Graded reduction of Pafah1b1 (Lis1) activity results in neuronal migration defects and early embryonic lethality. Nat Genet. 1998; 19:333–339. [PubMed: 9697693]
5. Hattori M, Adachi H, Tsujimoto M, Arai H, Inoue K. Miller-Dieker lissencephaly gene encodes a subunit of brain platelet-activating factor acetylhydrolase [corrected]. Nature. 1994; 370:216–218. [PubMed: 8028668]
6. Vallee RB, Tai C, Faulkner NE. LIS1: cellular function of a disease-causing gene. Trends Cell Biol. 2001; 11:155–160. [PubMed: 11306294]
7. Wynshaw-Boris A. Lissencephaly and LIS1: insights into the molecular mechanisms of neuronal migration and development. Clin Genet. 2007; 72:296–304. [PubMed: 17850624]
8. Yamada M, et al. LIS1 and NDEL1 coordinate the plus-end-directed transport of cytoplasmic dynein. Embo J. 2008; 27:2471–2483. [PubMed: 18784752]
9. Sasaki S, et al. Complete loss of Ndel1 results in neuronal migration defects and early embryonic lethality. Mol Cell Biol. 2005; 25:7812–7827. [PubMed: 16107726]
10. Hatten ME. Neuronal regulation of astroglial morphology and proliferation in vitro. J Cell Biol. 1985; 100:384–396. [PubMed: 3881455]
11. Tanaka T, et al. Lis1 and doublecortin function with dynein to mediate coupling of the nucleus to the centrosome in neuronal migration. J Cell Biol. 2004; 165:709–721. [PubMed: 15173193]
12. Toyo-Oka K, et al. Recruitment of katanin p60 by phosphorylated NDEL1, an LIS1 interacting protein, is essential for mitotic cell division and neuronal migration. Hum Mol Genet. 2005; 14:3113–3128. [PubMed: 16203747]
13. Schaller MD. Biochemical signals and biological responses elicited by the focal adhesion kinase. Biochim Biophys Acta. 2001; 1540:1–21. [PubMed: 11476890]
14. Parsons JT, Martin KH, Slack JK, Taylor JM, Weed SA. Focal adhesion kinase: a regulator of focal adhesion dynamics and cell movement. Oncogene. 2000; 19:5606–5613. [PubMed: 11114741]
15. Bhatt A, Kaverina I, Otey C, Huttenlocher A. Regulation of focal complex composition and disassembly by the calcium-dependent protease calpain. J Cell Sci. 2002; 115:3415–3425. [PubMed: 12154072]
16. Cuevas BD, et al. MEKK1 regulates calpain-dependent proteolysis of focal adhesion proteins for rear-end detachment of migrating fibroblasts. Embo J. 2003; 22:3346–3355. [PubMed: 12839996]
17. Serrano K, Devine DV. Vinculin is proteolyzed by calpain during platelet aggregation: 95 kDa cleavage fragment associates with the platelet cytoskeleton. Cell Motil Cytoskeleton. 2004; 58:242–252. [PubMed: 15236355]
18. Franco SJ, et al. Calpain-mediated proteolysis of talin regulates adhesion dynamics. Nat Cell Biol. 2004; 6:977–983. [PubMed: 15448700]
19. Xi X, et al. Tyrosine phosphorylation of the integrin beta 3 subunit regulates beta 3 cleavage by calpain. J Biol Chem. 2006; 281:29426–29430. [PubMed: 16935858]
20. Xie Z, Sanada K, Samuels BA, Shih H, Tsai LH. Serine 732 phosphorylation of FAK by Cdk5 is important for microtubule organization, nuclear movement, and neuronal migration. Cell. 2003; 114:469–482. [PubMed: 12941275]
21. Tsai LH, Delalle I, Caviness VS Jr, Chae T, Harlow E. p35 is a neural-specific regulatory subunit of cyclin-dependent kinase 5. Nature. 1994; 371:419–423. [PubMed: 8090221]
22. Tsai LH, Takahashi T, Caviness VS Jr, Harlow E. Activity and expression pattern of cyclin-dependent kinase 5 in the embryonic mouse nervous system. Development. 1993; 119:1029–1040. [PubMed: 8306873]

23. Goll DE, Thompson VF, Li H, Wei W, Cong J. The calpain system. Physiol Rev. 2003; 83:731–801. [PubMed: 12843408]
24. Suzuki K, Hata S, Kawabata Y, Sorimachi H. Structure, activation, and biology of calpain. Diabetes. 2004; 53 Suppl 1:S12–S18. [PubMed: 14749260]
25. Arthur JS, Elce JS, Hegadorn C, Williams K, Greer PA. Disruption of the murine calpain small subunit gene, Capn4: calpain is essential for embryonic development but not for cell growth and division. Mol Cell Biol. 2000; 20:4474–4481. [PubMed: 10825211]
26. Yingling J, et al. Neuroepithelial stem cell proliferation requires LIS1 for precise spindle orientation and symmetric division. Cell. 2008; 132:474–486. [PubMed: 18267077]
27. McEvilly RJ, de Diaz MO, Schonemann MD, Hooshmand F, Rosenfeld MG. Transcriptional regulation of cortical neuron migration by POU domain factors. Science. 2002; 295:1528–1532. [PubMed: 11859196]
28. Gressens P. Pathogenesis of migration disorders. Curr Opin Neurol. 2006; 19:135–140. [PubMed: 16538086]
29. Paylor R, et al. Impaired learning and motor behavior in heterozygous Pafah1b1 (Lis1) mutant mice. Learn Mem. 1999; 6:521–537. [PubMed: 10541472]
30. Amende I, et al. Gait dynamics in mouse models of Parkinson's disease and Huntington's disease. J Neuroeng Rehabil. 2005; 2:20. [PubMed: 16042805]
31. Powell E, Anch AM, Dyche J, Bloom C, Richtert RR. The splay angle: A new measure for assessing neuromuscular dysfunction in rats. Physiol Behav. 1999; 67:819–821. [PubMed: 10604857]
32. Bi W, et al. Increased LIS1 expression affects human and mouse brain development. Nat Genet. 2009; 41:168–177. [PubMed: 19136950]
33. Lee MS, et al. Neurotoxicity induces cleavage of p35 to p25 by calpain. Nature. 2000; 405:360–364. [PubMed: 10830966]
34. Patzke H, Tsai LH. Calpain-mediated cleavage of the cyclin-dependent kinase-5 activator p39 to p29. J Biol Chem. 2002; 277:8054–8060. [PubMed: 11784720]
35. Chae T, et al. Mice lacking p35, a neuronal specific activator of Cdk5, display cortical lamination defects, seizures, and adult lethality. Neuron. 1997; 18:29–42. [PubMed: 9010203]
36. Kasai Y, Inomata M, Hayashi M, Imahori K, Kawashima S. Isolation and characterization of monoclonal antibodies against calcium-activated neutral protease with low calcium sensitivity. J Biochem. 1986; 100:183–190. [PubMed: 3020013]
37. Lindsay RM. Nerve growth factors (NGF, BDNF) enhance axonal regeneration but are not required for survival of adult sensory neurons. J Neurosci. 1988; 8:2394–2405. [PubMed: 3249232]
38. Tabata H, Nakajima K. Efficient in utero gene transfer system to the developing mouse brain using electroporation: visualization of neuronal migration in the developing cortex. Neuroscience. 2001; 103:865–872. [PubMed: 11301197]
39. Saito T, Nakatsuji N. Efficient gene transfer into the embryonic mouse brain using in vivo electroporation. Dev Biol. 2001; 240:237–246. [PubMed: 11784059]
40. Yamasaki N, et al. Alpha-CaMKII deficiency causes immature dentate gyrus, a novel candidate endophenotype of psychiatric disorders. Mol Brain. 2008; 1:6. [PubMed: 18803808]
41. Hampton TG, Stasko MR, Kale A, Amende I, Costa AC. Gait dynamics in trisomic mice: quantitative neurological traits of Down syndrome. Physiol Behav. 2004; 82:381–389. [PubMed: 15276802]

Figure 1a-b

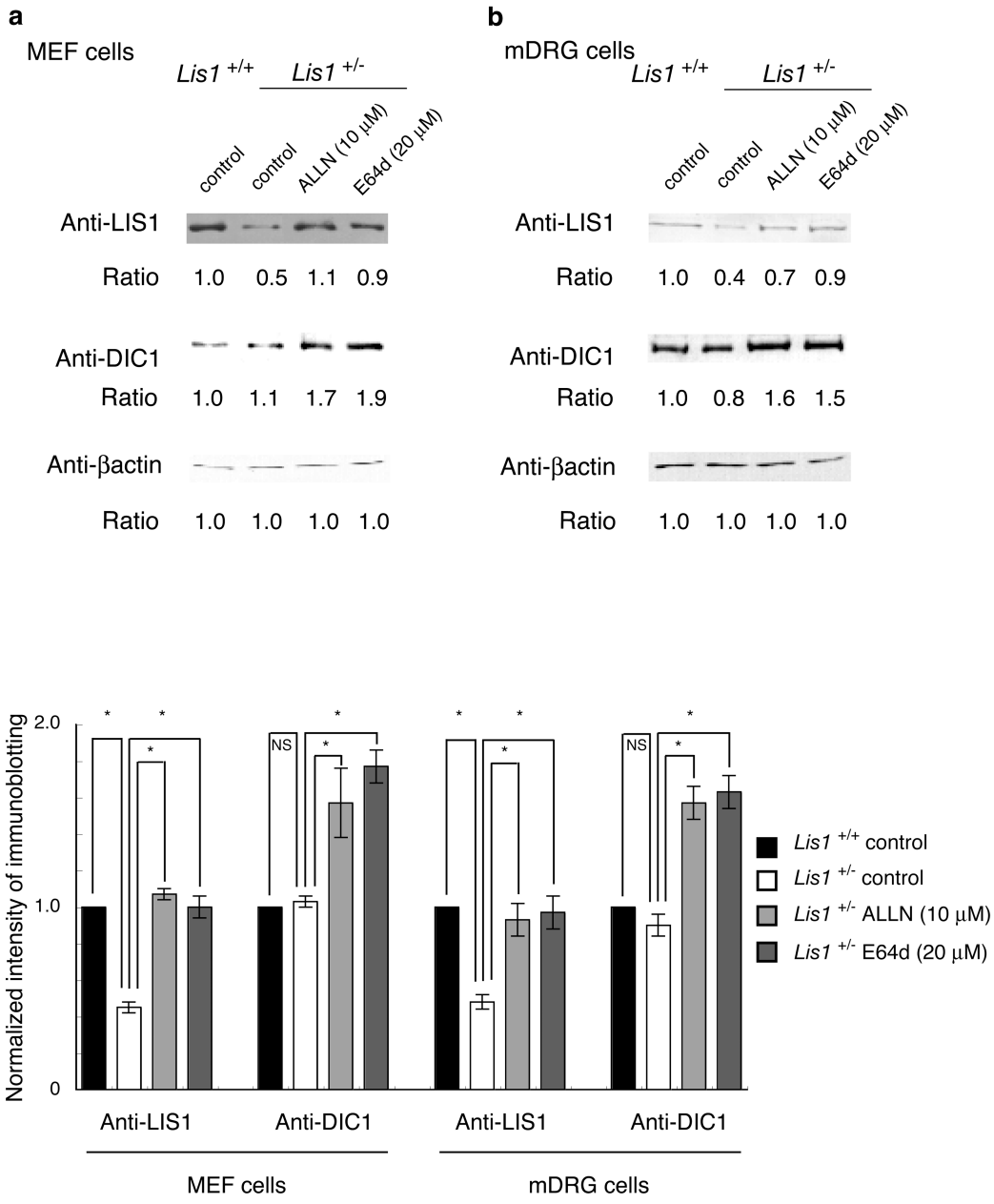

Figure 1. Western blotting analysis and distribution of LIS1, dynein intermediate chain (DIC1), and cellular components after administration of calpain inhibitors in MEF cells

We examined LIS1 or DIC1 protein level after administration of 10 μM ALLN or 20 μM E64d by Western blotting in mouse embryonic fibroblast (MEF) cells **(a)** or dorsal root ganglia (DRG) neurons **(b)**. Western blotting was performed 2 hrs after the start of treatment. Protein levels were normalized by comparison with the β-actin control and are indicated at the bottom of each panel. Statistical examination was performed by unpaired Student's *t*-test, which is shown at the bottom, with *P<0.05. Error bars in graphs were expressed as mean±SEM. We performed three independent sets of experiments. One

representative data set is shown. Note: LIS1 and DIC1 were augmented by ALLN or E64d treatment.

Figure 2a-b

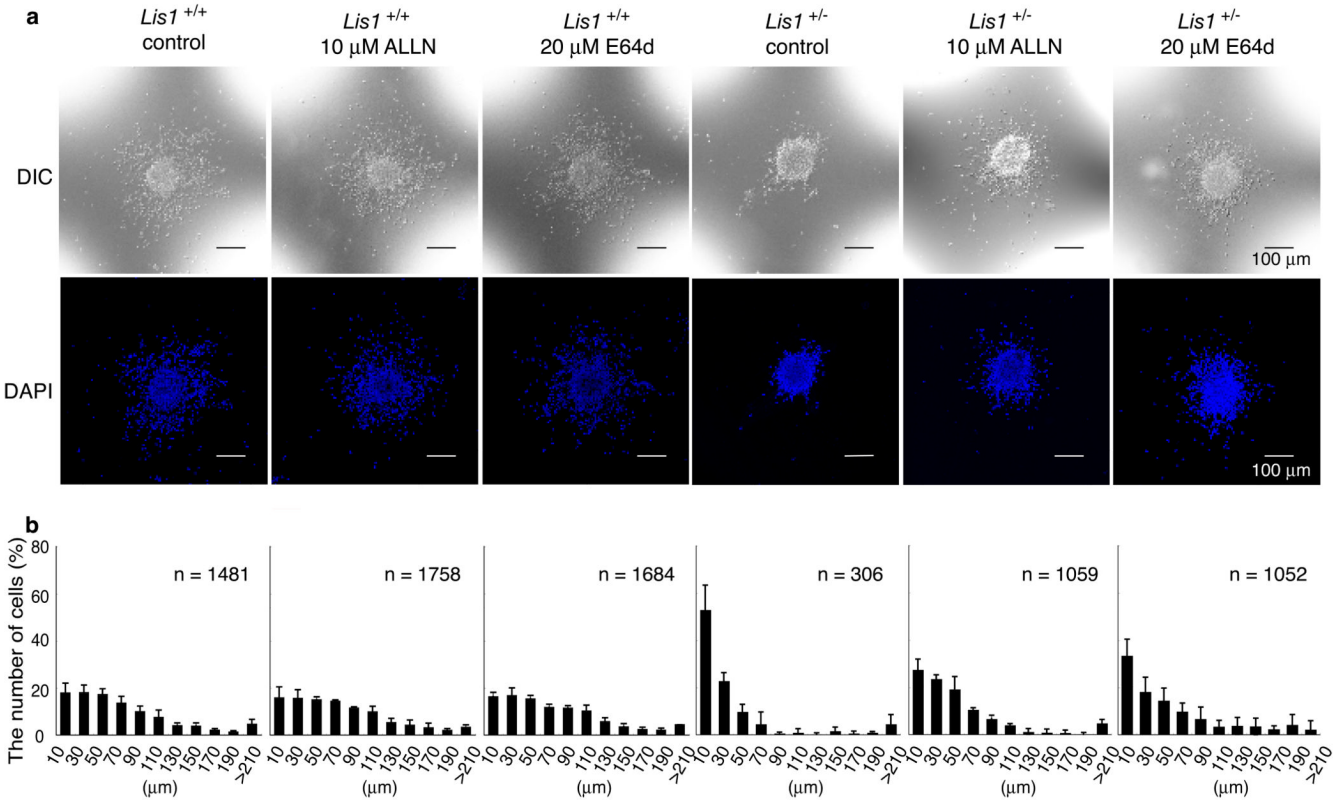

Figure 2c

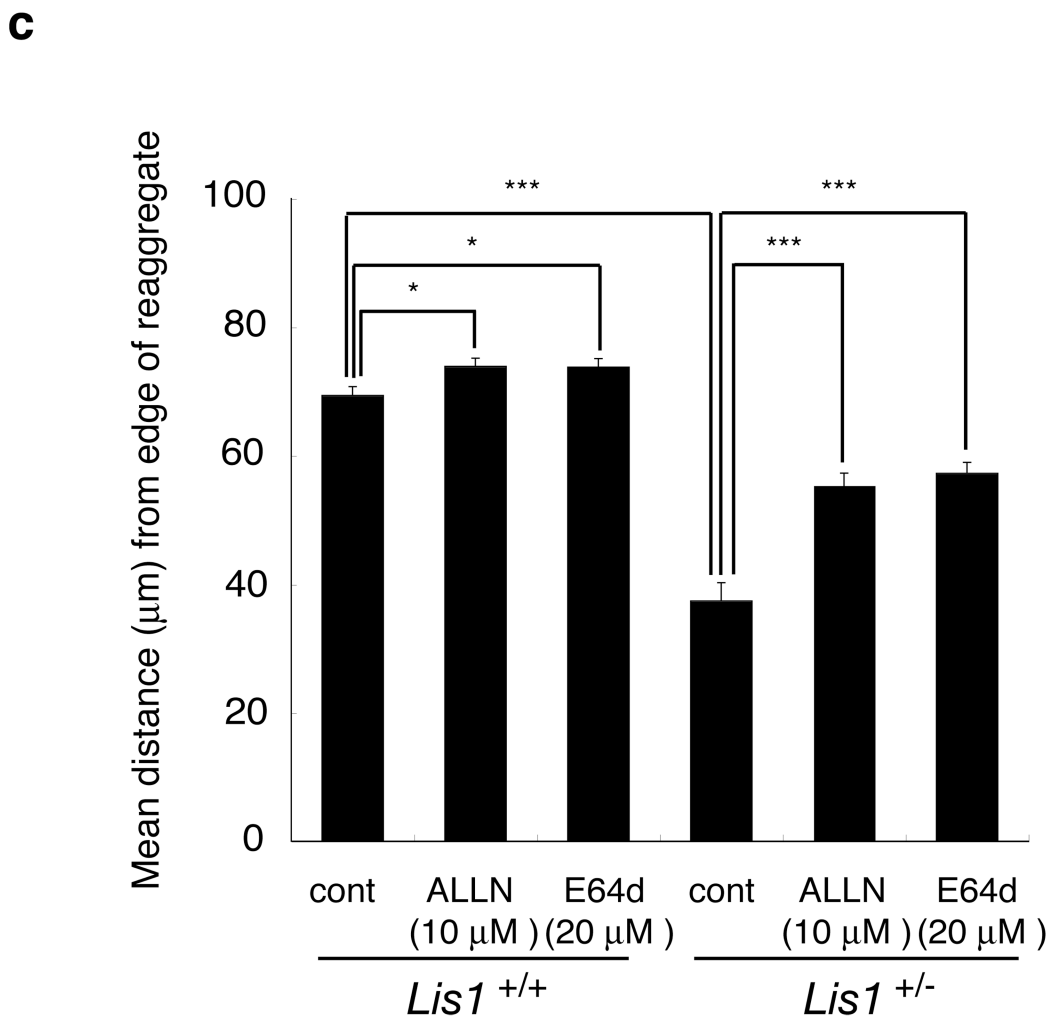

Figure 2. Rescue of neuronal migration by administration of calpain inhibitors

Migration assay using cerebellar granule neurons. Images of granule neuron clusters are shown **(a)**. The migration distance of each neuron 16 hrs after 10 μM ALLN or 20 μM E64d treatment was binned **(b)**. Wild type neurons displayed normal migration distances, whereas *Lis1+/−* neurons displayed a shift in the distribution of bins toward the left. *Lis1+/−* neurons in the presence of 10 μM ALLN or 20 μM E64d clearly showed improvement of migration defects. Mean migration distances are summarized at the bottom **(c)**. *n* is the number of neurons measured for each examination. Statistical analysis was performed by the unpaired Student's *t*-test, with *P<0.05 and ***P<0.001. Error bars in graphs were expressed as mean ±SEM. We performed three independent sets of experiments, and obtained reproducible results. Note; calpain inhibitors moderately facilitated neuronal migration in wild type cells, and rescued defective neuronal migrations in *Lis1+/−* neurons.

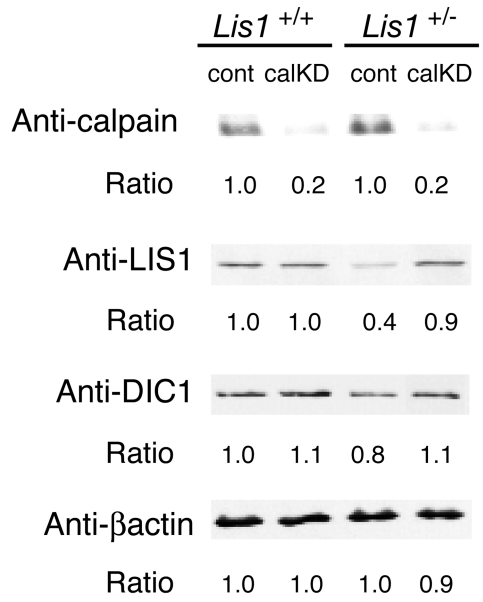

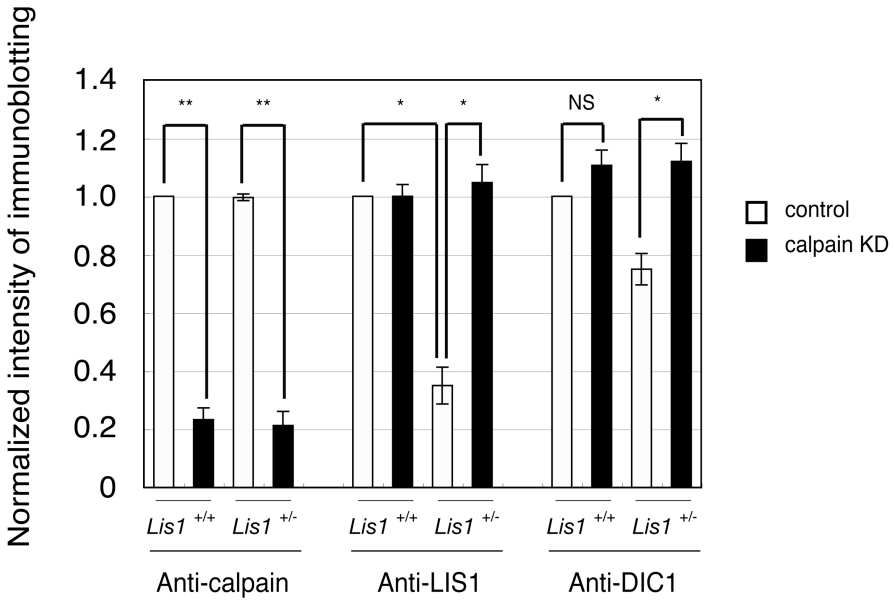

Figure 3. Knockdown of calpain by siRNA

MEF cells were transfected with siRNA against calpain small subunit 1 (*Capns1*). Western blotting was performed 120 hrs after transfection of siRNA. Note: depletion of calpain small subunit 1 resulted in reduction of μ-calpain and m-calpain accompanied by increase of LIS1 and DIC1. Statistical analysis was performed by the unpaired Student's *t*-test, which is shown at the bottom, with *P<0.05 or **P<0.01. We performed three independent sets of experiments. One representative data set is shown.

Figure 4a-b

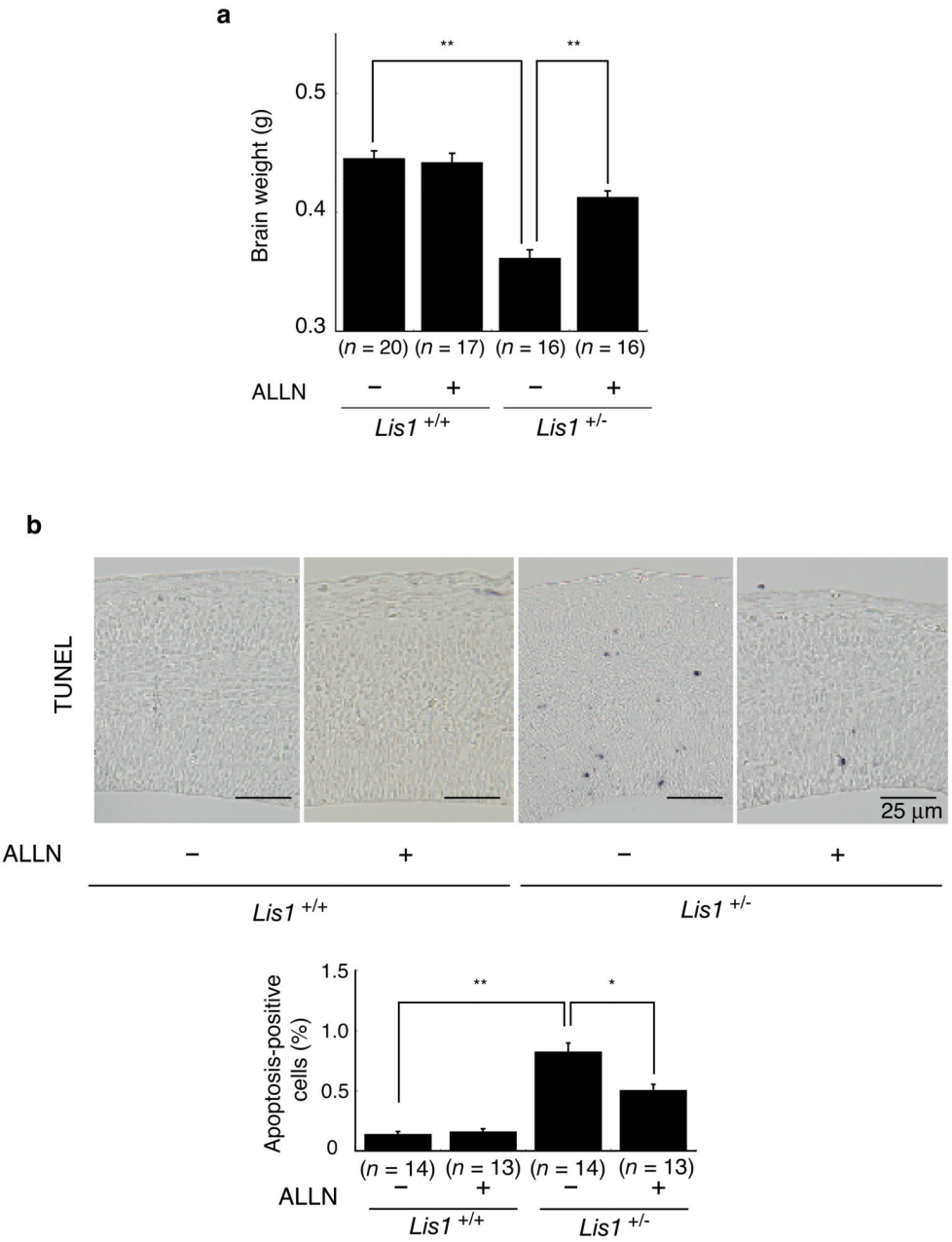

Figure 4c-d

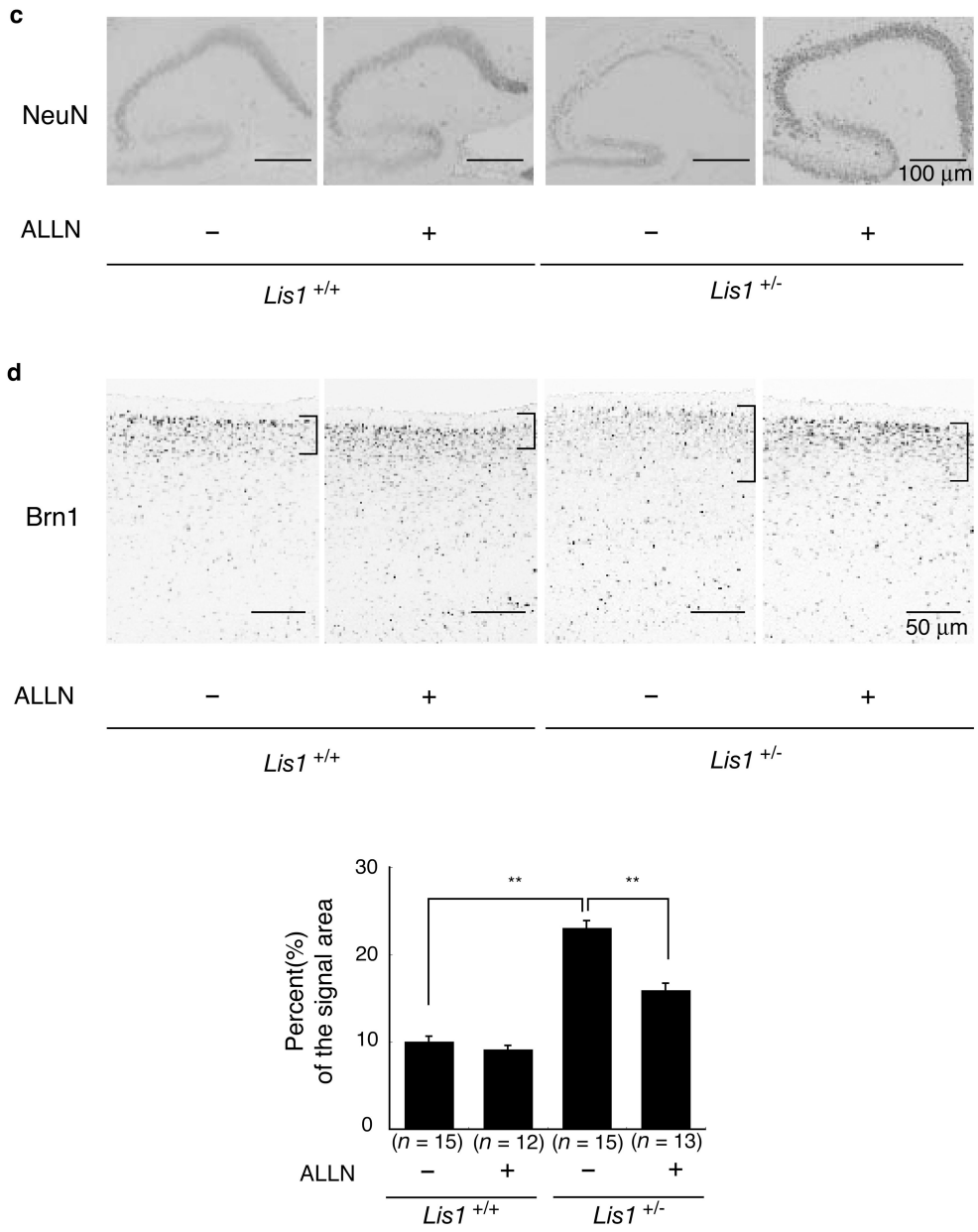

Figure 4e

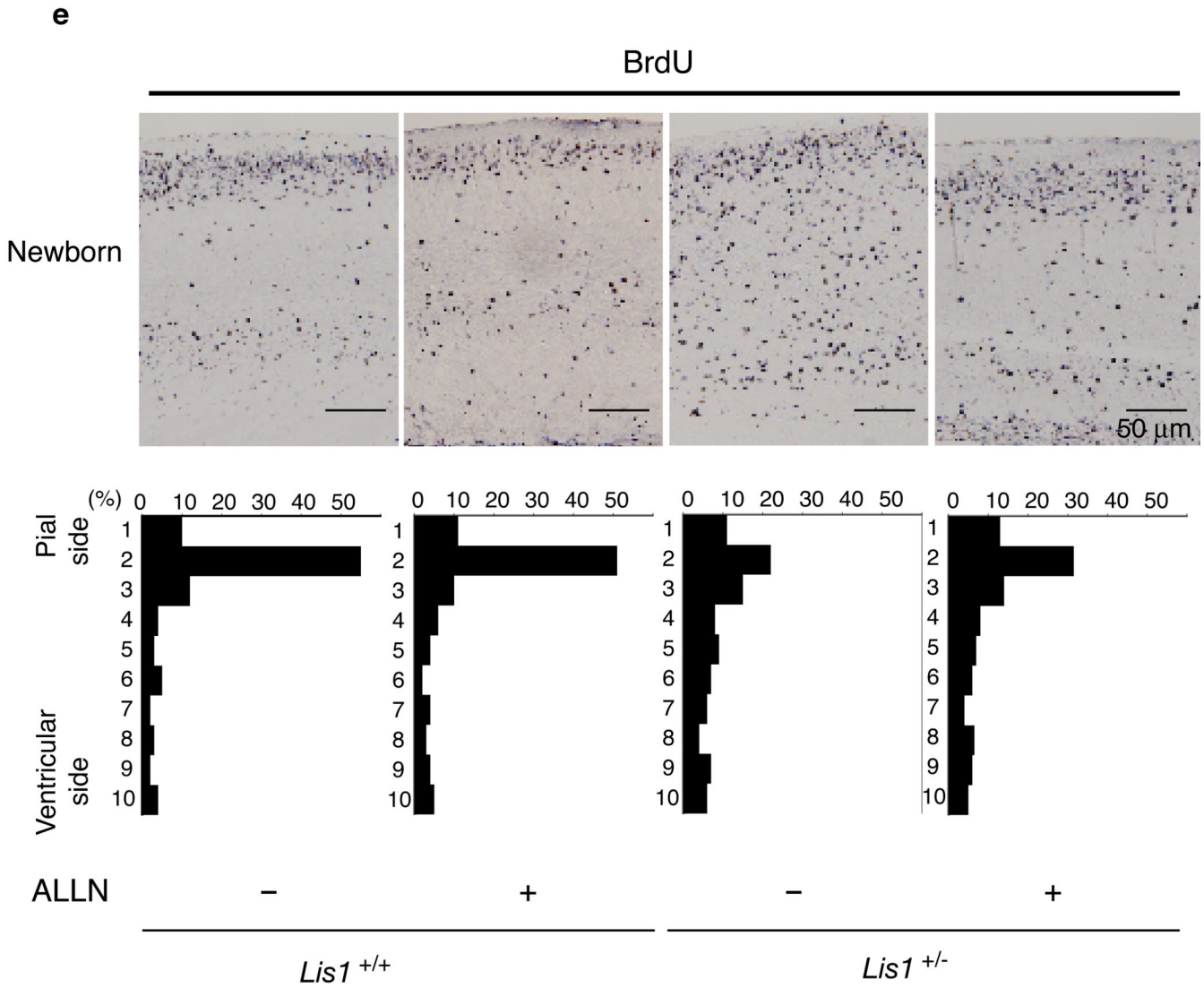

Figure 4f

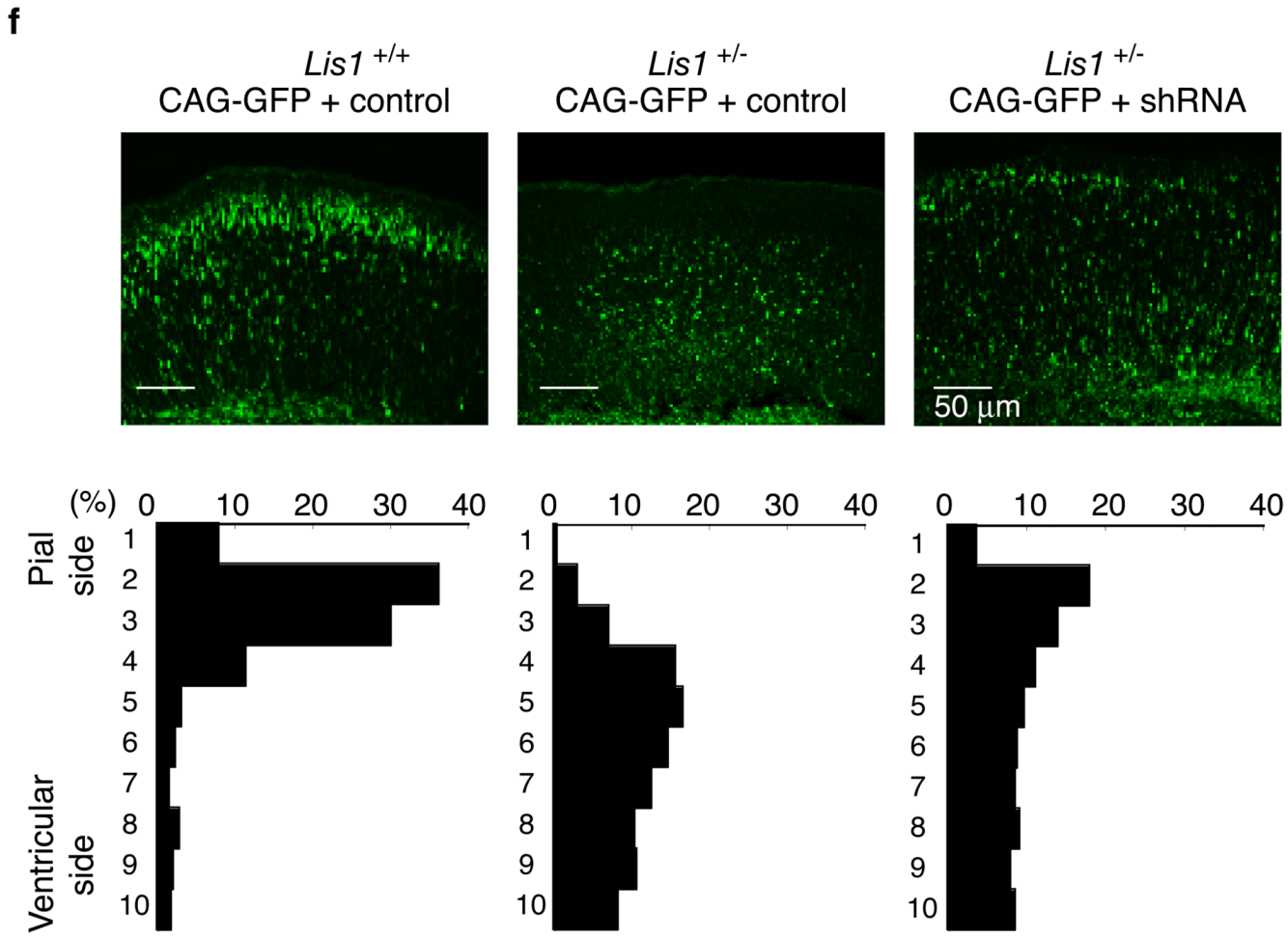

Figure 4. Rescue of defective corticogenesis in *Lis1*+/− mice by intra-peritoneal injection of ALLN

(a) Measurement of brain weight at d5. Genotyping and injection of ALLN are indicated at the bottom. *n* is the number of brains examined. All statistical analyses were performed by the unpaired Student's *t*-test. Error bars: ±SEM. Statistical significance was defined as *P<0.05 or **P<0.01. **(b)** Apoptotic cell death was examined by TUNEL staining at E15.5. Histogram plots of the relative frequency of TUNEL positive cell to the total number of cells are shown at the bottom. *n* is the number of brains examined. Error bars: ±SEM. **(c)** Neu-N staining of mid-sagittal sections of the hippocampus is shown. Severe cell dispersion and splitting of CA3 region were observed in the *Lis1*+/− mouse. **(d)** Cortical phenotypes were examined by a layer specific maker, Brn-1 (layer 2 and 3). The distribution of Brn-1 positive cells is indicated at the right side of each panel. Quantitation of the thickness of Brn-1 positive cells is summarized at the bottom. *n* is the number of brains examined. Error bars: ±SEM. **(e)** BrdU birthdating analysis Quantitative analysis was performed by measuring the

distribution of BrdU labeled cells in each bin that equally divided the cortex from ML to SP. **(f)** *In utero* injection of shRNA against *Capns1*. The distribution of migrated neurons is shown at lower panels. Cortex was divided into ten compartments, followed by counting of the neurons located at each compartment, and summarized.

Figure 5a-d

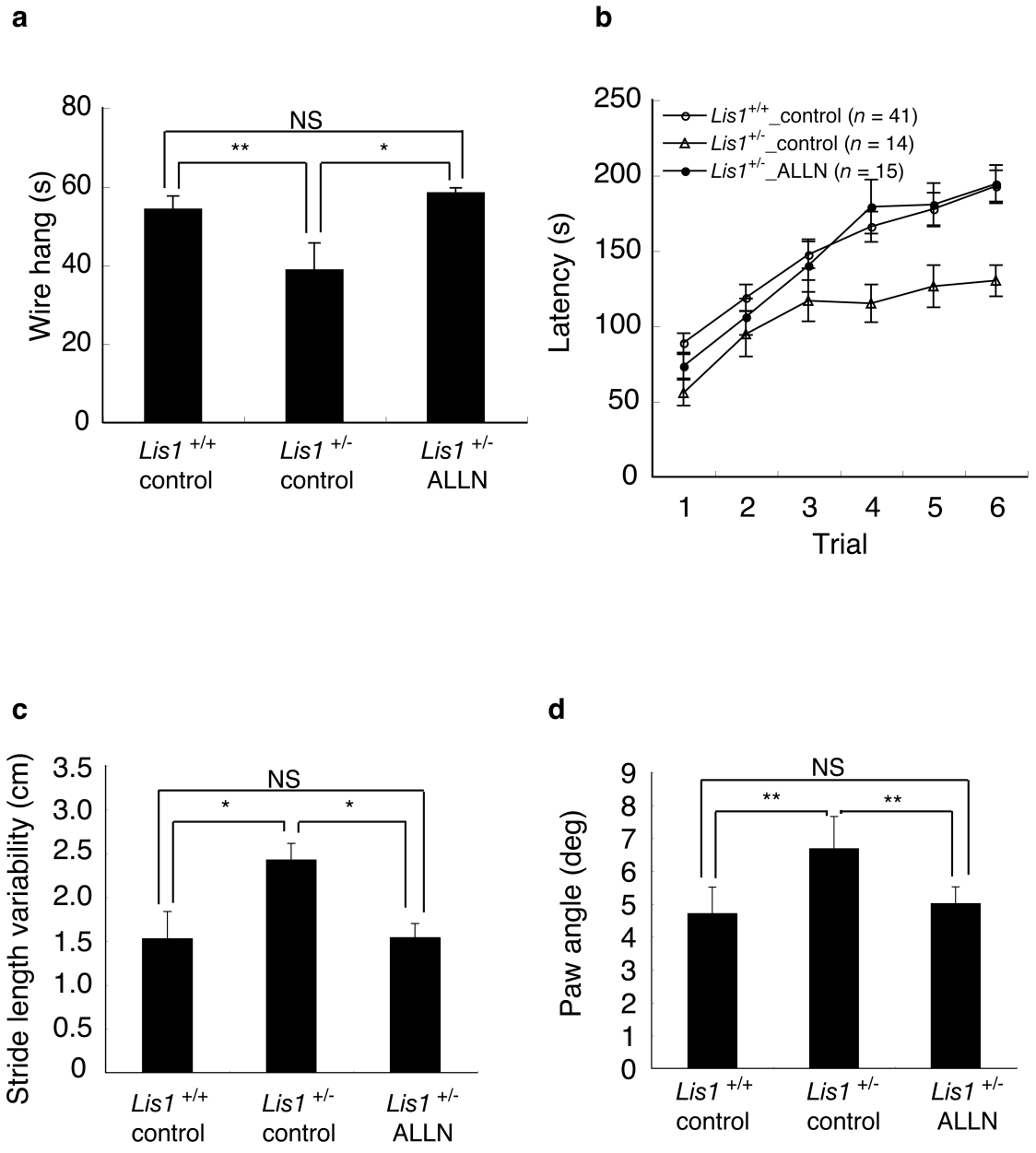

Figure 5. Rescue of impaired behavior in *Lis1*+/− mice by intra-peritoneal injection of ALLN

Neurological screen: wire hang test **(a)**. Note: there were no obvious differences in body weight, rectal temperature (Supplementary Table 1) and grip strength in each group. *Lis1+/−* mice displayed clear shorter time to falling in the wire hang test. P-values are shown at the upper parts of bars. Statistical analysis was conducted using Stat View (SAS institute). Data were analyzed by two-way ANOVA. Error bars in graphs were expressed as mean±SEM. All P-values indicated are two tailed. Statistical significance was defined as *P<0.05 or **P<0.01. **(b)** Examination of motor function by the rotarod test. Time spent balanced on top of the rotating rod was measured across six test trials for *Lis1+/+* mice (open circle),

Lis1+/− mice without ALLN treatment (open triangle) and *Lis1+/−* mice with ALLN treatment (closed circle). Significant differences between *Lis1+/+* mice and *Lis1+/−* mice (***P<0.001) were observed. *Lis1+/−* mice with ALLN treatment displayed improvement of rotarod performance. Data were analyzed by two-way repeated measures. **(c)** Examination of stride length variability and **(d)** fore paw angle in gait analysis. *Lis1+/−* mice with ALLN treatment displayed improvement of gait parameters. Data were analyzed by two-way ANOVA.